A KF-BASED LOCALIZATION ALGORITHM FOR NONHOLONOMIC MOBILE ROBOTS

E. FABRIZI, G. ORIOLO

Dip. di Informatica e Sistemistica, Università di Roma "La Sapienza", Via Eudossiana 18, 00184 Roma, Italy
E-mail: fabrizi@labrob.ing.uniroma1.it, oriolo@labrob.ing.uniroma1.it

S. PANZIERI, G. ULIVI

Dip. di Informatica e Automazione, Universit di Roma Tre, Via della Vasca Navale 79, 00146 Roma, Italy
E-mail: panzieri@uniroma3.it, ulivi@uniroma3.it

We address the localization problem in unstructured environments for a nonholonomic mobile robot equipped with exteroceptive sensors. The usual approach to robot localization is to adopt the Extended Kalman Filter (EKF), which results in a typical predictor-corrector structure. The use of the EKF, as opposed to the standard Kalman Filter, derives from the nonlinearity of the robot kinematic model as well as of the observation function. In order to avoid at least the first linearization error, we propose to take advantage of the possibility of transforming the original kinematic system in chained form through an appropriate feedback transformation. The obtained equations are closed-form integrable, thereby yielding a linear discrete-time model which provides exact odometric prediction and associated covariance. Another advantage of our approach is that the stochastic description of the noise in the chained-form coordinates is more natural. The performance of the proposed localization method is illustrated through simulations on a mobile robot having the kinematics of a unicycle and equipped with ultrasonic sensors.

1 Introduction

The subject of this paper is the localization problem for a nonholonomic mobile robot equipped with exteroceptive sensors. Without a specific localization capability, a mobile robot should only rely on odometry, i.e., on its kinematic model to update its location estimate (*dead reckoning*). However, due to slippage, wheel misalignment, and other non-idealities, such a mode of operation invariably results in the accumulation of large errors, and eventually in the robot 'getting lost' after a sufficiently long path. Hence, efficient localization requires that the robot exploits the information coming from its exteroceptive sensors (e.g., range finders, vision systems).

Most localization methods are based on the principle of performing a comparison between the actual exteroceptive sensor measures and their value as predicted on the basis of the a priori knowledge of the environment (e.g., a map). The outcome of this comparison can be either used to correct the location estimate produced by the odometric system, or to directly assess a new estimate for the robot location.[1–9] In structured environments, one can use beacons or easily recognizable markers as environment features. In unstructured environments, however, the localization algorithm should exploit "natural" features, e.g., the obstacles that are present in the workspace.

In this context, the most common approach to integrate uncertain information coming from various sources is to adopt the Extended Kalman Filter (EKF), which results in a typical predictor-corrector structure.[2,5,6,8] The use of the EKF, as opposed to the standard Kalman Filter, derives from the necessity of dealing with a nonlinear kinematic model of the robot to determine an odometric position prediction and the associated uncertainty, represented by a covariance matrix, as well as from the nonlinearity of the outputs (sensor measures) with respect to the robot state.

In order to limit the approximation error due to the linearization procedures included in the EKF, we propose to take advantage of the possibility of transforming the original kinematic system in chained form through an appropriate feedback transformation. The obtained equations are closed-form integrable, thereby providing a linear discrete-time model. Hence, it is possible to compute exactly the odometric prediction and the associated covariance matrix, without resorting to linear approximation. Another advantage of our approach is that a stochastic description of the noise in the chained-form coordinates appears to be more natural, because uncertainties are expressed in a frame attached to the robot body. The performance of the proposed localization method is compared with that of a conventional EKF-based algorithm through simulations on a mobile robot having the kinematics of a unicycle and equipped with ultrasonic sensors.

2 Chained-form representation of a unicycle

Consider a mobile robot with the kinematics of a unicycle. The robot generalized coordinates are given by the vector $x = (x_1, x_2, x_3) = (p_x, p_y, \theta)$, where p_x, p_y are the cartesian coordinates of the wheel axle midpoint in

a fixed world frame and θ is the orientation angle between the axle and the horizontal axis. The kinematic (*odometric*) model of the robot is

$$\begin{aligned} \dot{x}_1 &= u_1 \cos x_3 \\ \dot{x}_2 &= u_1 \sin x_3 \\ \dot{x}_3 &= u_2, \end{aligned} \tag{1}$$

where the control inputs u_1 and u_2 are the linear and angular velocity, respectively. Such system is the simplest example of nonholonomic mobile robot.

With the following change of coordinates $\xi = \phi(x)$

$$\begin{aligned} \xi_1 &= -x_3 \\ \xi_2 &= x_1 \cos x_3 + x_2 \sin x_3 \\ \xi_3 &= x_2 \cos x_3 - x_1 \sin x_3 \end{aligned} \tag{2}$$

and transformation of inputs $v = \psi(x, u)$

$$\begin{aligned} v_1 &= -u_2 \\ v_2 &= u_1 + (x_2 \cos x_3 - x_1 \sin x_3) u_2 = u_1 + \xi_3 u_2, \end{aligned} \tag{3}$$

the system equations take the form

$$\begin{aligned} \dot{\xi}_1 &= v_1 \\ \dot{\xi}_2 &= v_2 \\ \dot{\xi}_3 &= \xi_2 v_1, \end{aligned} \tag{4}$$

referred to as a $(2,3)$ *chained form*.[10]

The new coordinates defined by eqs. (2) have an interesting interpretation. In fact, ξ_2 and ξ_3 are the cartesian coordinates of the robot in a moving reference frame, with the same origin of the world frame but rotated so as to align the ξ_2 axis with the vehicle orientation $x_3 = -\xi_1$.

Assume now that the unicycle moves along a trajectory under the action of nominal inputs $u_1(t)$ and $u_2(t)$, which may be assumed to take constant values $u_{1,k}$ and $u_{2,k}$, respectively, within the sampling interval $[kT, (k+1)T]$. Through the input transformation (3), these are converted to the values of the chained-form inputs $v_1(t)$ and $v_2(t)$. In particular, $v_1(t) = -u_{2,k}$ for $t \in [kT, (k+1)T]$, while v_2 is *not* constant during a sampling interval.

The simple form of eqs. (4) makes possible their exact integration. Letting $\xi_k = \xi(kT)$, a tedious but simple calculation yields the following *sampled dynamics* is derived

$$\begin{aligned} \xi_{1,k+1} &= \xi_{1,k} - T u_{2,k} \\ \xi_{2,k+1} &= \xi_{2,k} \cos(T u_{2,k}) + \xi_{3,k} \sin(T u_{2,k}) \\ &\quad + u_{1,k} \frac{\sin(T u_{2,k})}{u_{2,k}} \\ \xi_{3,k+1} &= \xi_{3,k} \cos(T u_{2,k}) - \xi_{2,k} \sin(T u_{2,k}) \\ &\quad + u_{1,k} \frac{\cos(T u_{2,k}) - 1}{u_{2,k}}. \end{aligned}$$

In compact form, the above model is written as

$$\xi_{k+1} = A_k \xi_k + v_k, \tag{5}$$

having defined

$$A_k = \begin{pmatrix} 1 & 0 & 0 \\ 0 & \cos(T u_{2,k}) & \sin(T u_{2,k}) \\ 0 & -\sin(T u_{2,k}) & \cos(T u_{2,k}) \end{pmatrix}$$

and a new input vector

$$v_k = \begin{pmatrix} -T u_{2,k} \\ u_{1,k} \frac{\sin(T u_{2,k})}{u_{2,k}} \\ u_{1,k} \frac{\cos(T u_{2,k}) - 1}{u_{2,k}} \end{pmatrix}.$$

The sampled dynamic model (5) is a linear discrete-time system that allows to compute exactly the robot transformed coordinates ξ at each sampling instant. By inverting eqs. (2), these can be converted to the corresponding value of the world-frame coordinates x.

3 A perturbed kinematic model

In practice, use of the kinematic model (1) to compute the current robot position from the knowledge of the applied inputs $u_{1,k}$ and $u_{2,k}$ results in errors that increase over time. This is due to various factors, the most relevant being wheel slippage. When this phenomenon occurs, the kinematic model (1) does not apply, for the latter is derived under the *rolling without slipping* assumption. Other nonidealities include wheel misalignment, tire deformations and external disturbances (e.g., wind or gravity).

The above situation is usually represented by introducing state perturbations on the kinematic model (1). In our case, this can be done with reference to the discrete-time system (5), thereby obtaining the following perturbed model

$$\xi_{k+1} = A_k \xi_k + v_k + n_k, \tag{6}$$

where n_k is assumed to be a zero-mean gaussian noise with diagonal covariance matrix Q_k.

In view of the coordinate transformation (2), the first element of the diagonal of Q_k represents the uncertainty on robot orientation, while the other two elements describe the cartesian position uncertainty. It should be emphasized how the use of ξ coordinates results in a more natural stochastic characterization of errors, because uncertainties are expressed in a frame attached to the robot body. In particular, from a geometric point of view, matrix Q_k represents an ellipsoid in the robot frame.

If the robot is equipped with an exteroceptive sensory system which provides a vector of range readings z,

we can associate an output (*observation*) function to the model:

$$z_{k+1} = h(x_{k+1}, \mathcal{M}),$$

where $\mathcal{M}$ is the environment description (typically, a map). It should be noted that h reflects the structure of the environment as well as the (geometric) model of interaction between the environment itself and the sensors. In general, however, function h is highly nonlinear.

Since most sensors are noisy—this is particularly true for ultrasonic transducers—it is appropriate to consider a perturbed output equation

$$z_{k+1} = h(x_{k+1}, \mathcal{M}) + w_k, \tag{7}$$

with w_k a zero-mean gaussian observation noise with diagonal covariance matrix R_k.

4 Structure of the localization algorithm

The structure of most localization systems proceeds directly from the EKF equations.[11] Our approach (see Fig. 1) is based on the same conceptual framework, but it differs in the extensive use of the linear sampled dynamics (5) in place of the nonlinear kinematic model (1).

At the $(k+1)$-th step, eqs. (5) are used in order to compute an odometric position prediction ($\hat{\xi}_{k+1/k}$) and an associated covariance matrix ($P_{k+1/k}$). On the basis of the environment map, an observation prediction $\hat{z}_{k+1}$ is formed from $\hat{\xi}_{k+1/k}$ and compared with the actual sensor readings z_{k+1}. The results are the innovation term (ν_{k+1}) and its covariance matrix (S_{k+1}), that are used by the EKF to produce the final position estimate ($\hat{\xi}_{k+1}$) and the associated covariance (P_{k+1}).

In the remainder of this section, each phase is described in some detail.

Odometric prediction

The odometric prediction, denoted by $\hat{\xi}_{k+1/k}$, is obtained by computing the sampled dynamics (5) on the basis of the nominal inputs. In formulas:

$$\hat{\xi}_{k+1/k} = A_k \xi_k + v_k.$$

The covariance matrix associated with the odometric prediction is updated as

$$P_{k+1/k} = A_k P_k A_k^T + Q_k,$$

in view of the linearity of system (5). Here, P_k is the covariance matrix of the final prediction computed at the previous time instant.

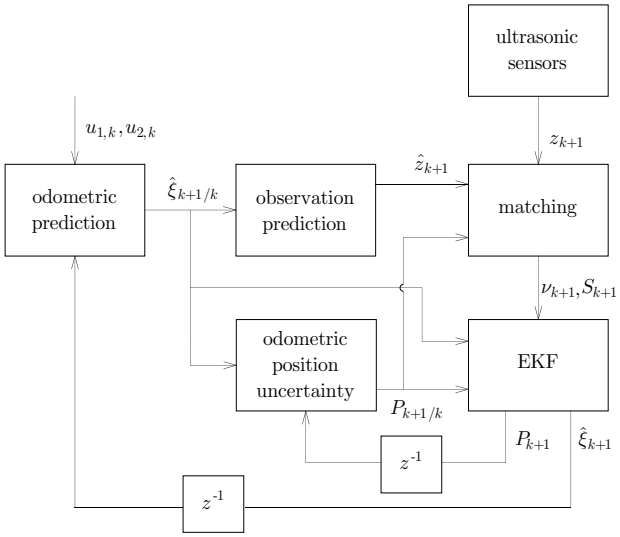

Figure 1: Structure of the localization system (z^{-1} denotes the unit delay operator).

Observation prediction and matching

In this phase, the environment map $\mathcal{M}$ and the odometric prediction $\hat{\xi}_{k/k-1}$ are first used to generate a vector of predicted range readings $\hat{z}_k$ (one reading for each sonar):

$$\hat{z}_{k+1} = h(\hat{\xi}_{k+1/k}, \mathcal{M}).$$

To perform this computation, the observation function h must be expressed in the moving frame coordinates ξ.

The *innovation* term is defined as follows

$$\nu_{k+1} = z_{k+1} - \hat{z}_{k+1}.$$

Due to the nonlinearity of the output function, the associated covariance is computed as[1]

$$S_{k+1} = J_\xi^h(\hat{\xi}_{k+1/k}) P_{k+1/k} (J_\xi^h(\hat{\xi}_{k+1/k}))^T + R_k,$$

where $J_\xi^h(\cdot)$ is the Jacobian matrix of h with respect to ξ. Note that the first term of S_{k+1} represents the uncertainty on the observation due to the uncertainty on the odometric prediction.

To avoid the inclusion of erroneous measures (*outliers*) in the correction phase, it is advisable to set up a *validation gate* as follows.[2] The innovation term for the j-th sensor $\nu_{k+1,j}$ (i.e., the j-th component of ν_{k+1}) is passed to the filter only if

$$\frac{\nu_{k+1,j}^2}{s_{k+1,j}} \leq \beta^2, \tag{8}$$

where s_j is the j-th diagonal term of S_{k+1} and parameter β should be tuned by experimental trials. Measures which fail to satisfy (8) are ignored by the EKF.

Extended Kalman Filter

At this stage, the Extended Kalman Filter is used to correct the odometric position estimate on the basis of validated observations. Note that, although the discrete-time system (6) is linear, it is nonetheless necessary to resort to the EKF equations in view of the nonlinearity of the observation function.

In particular, the final position estimate in the ξ coordinates is obtained as

$$\hat{\xi}_{k+1} = \hat{\xi}_{k+1/k} + K_{k+1}\nu_{k+1},$$

where K_{k+1} is the Kalman gain matrix

$$K_{k+1} = P_{k+1/k}J_{\xi}^{h}(\hat{\xi}_{k+1/k})S_{k+1}^{-1}.$$

The covariance matrix associated with the position estimate ξ_{k+1} is given by

$$P_{k+1} = P_{k+1/k} - K_{k+1}S_{k+1}K_{k+1}^{T}.$$

Finally, the reconstructed position in the world frame is computed as

$$\hat{x}_{k+1} = \phi^{-1}(\hat{\xi}_{k+1}).$$

5 Simulation Results

To assess the performance of the proposed localization method, we have compared by simulation its results with those of a conventional EKF-based algorithm. The considered vehicle has two driving wheels and is equipped with five ultrasonic sensors with a radiation cone of about 80°. The first sonar is oriented in the forward direction, while the other two couples make an angle of $\pm 55°$ and $\pm 90°$, respectively, with the forward axis. The resulting system models a robotized wheelchair prototype built at the robotics lab of the Universit di Roma Tre, on which we intend to implement our method.

The simulated environment (see Fig. 2) is a long corridor with a broadening in the center and a right turn in the second half. The length of the path followed by the robot is about 20 meters. The average speed of the robot is 0.3 m/s, while ultrasonic measures are collected every $T = 0.5$ sec. The control inputs u_1 and u_2 are constant within each sampling period; as a consequence, nominal trajectories are made of linear and circular tracts. The actual path of the robot, shown in triangles, was obtained via the perturbed model (6), with n a zero-mean gaussian noise with covariance matrix $Q = \text{diag}\{0.0001, 0.001, 0.0001\}$. Note in particular the severe lateral slippage occurring during the last right turn. As in eq. (7), simulated sonar readings are affected by a zero-mean gaussian noise w with covariance matrix $R = \text{diag}\{0.01, 0.01, 0.01, 0.01, 0.01\}$.

Figure 2 shows the results obtained with our proposed method: the odometric position estimate is shown dotted, while the path reconstructed by the localization algorithm is shown as a solid line. Note the satisfactory accordance between the latter and the actual path, even in correspondence to slippage phases.

To allow a comparison, the outcome of a conventional EKF-based localization algorithm [2] is shown in Fig. 3. In this case, filter equations were obtained by using the nonlinear odometric model (1); in particular, the state error covariance matrix was obtained by transforming in cartesian coordinates the ellipsoid represented by Q. The resulting odometric position estimate (dots) is virtually coincident with that of our method. However,the reconstructed path (solid) appears to be less accurate; in particular, it tends to 'smooth' the actual path, particularly during slippage phases.

The improvement gained with our method is more appreciable by examining Figs. 4–7. The first two show the cartesian position error of both localization methods, while orientation errors are plotted in the last two. In general, our method achieves smaller error than conventional EKF-based localization. In particular, note the remarkable reduction of the orientation error (Figs. 6–7).

6 Conclusion

We have presented a localization method based on Kalman filtering theory for nonholonomic mobile robots. The innovative aspect of our technique with respect to existing methods stand in the use of a chained-form representation for the robot kinematics, leading to an exact sampled dynamic model which is linear. As a consequence, the odometric position prediction and the associated covariance matrix can be computed without resorting to linearization procedures. Moreover, the stochastic description of the noise in the chained-form coordinates appears to be more natural, because uncertainties are expressed in a frame attached to the robot body. The performance of our method has been demonstrated through simulations on a unicycle robot equipped with five ultrasonic sensors.

We are currently beginning the experimental validation of this method on a robotized wheelchair. Among the possible future directions of research, we mention the application of this approach to mobile robots with more complex but still chained-form transformable kinematic models as well as a closer investigation of the stochastic characteristics of the observation noise.

Acknowledgments

This work was partially supported by ENEA (*Antartica* national research program).

References

1. P. Moutarlier and R. Chatila, "An experimental system for incremental environment modelling by an autonomous mobile robot," *1st Int. Symp. on Experimental Robotics*, Montreal, CND, pp. 327–346, 1989.
2. J. J. Leonard and H. F. Durrant-Whyte, "Mobile robot localization by tracking geometric beacons," *IEEE Trans. on Robotics and Automation*, vol. 7, no. 3, pp. 376–382, 1991.
3. J. Gonzalez, A. Stentz, and A. Ollero, "An iconic position estimator for a 2D laser rangefinder," *1992 IEEE Int. Conf. on Robotics and Automation*, Nice, F, pp. 2646–2651, 1992.
4. S. Atiya and G. D. Hager, "Real-time vision-based robot localization," *IEEE Trans. on Robotics and Automation*, vol. 9, no. 6, pp. 785–800, 1993.
5. A. A. Holenstein and E. Badreddin, "Mobile-robot position update using ultrasonic range measurements," *Int. J. of Robotics and Automation*, vol. 9, no. 2, pp. 72–80, 1994.
6. B. Triggs, "Model-based sonar localisation for mobile robots," *Robotics and Autonomous Systems*, vol. 12, pp. 173–186, 1994.
7. P. MacKenzie and G. Dudek, "Precise positioning using model-based maps," *1994 IEEE Int. Conf. on Robotics and Automation*, San Diego, CA, pp. 1615–1621, 1994.
8. H. F. Durrant-Whyte, "Where am I? A tutorial on mobile vehicle localization," *Industrial Robot*, vol. 21, no. 2, pp. 11–16, 1994.
9. G. Fortarezza, G. Oriolo, G. Ulivi, M. Vendittelli, "A mobile robot localization method for incremental map building and navigation," *3rd Int. Symp. on Intelligent Robotic Systems*, Pisa, I, pp. 57-65, 1995.
10. R. M. Murray and S. S. Sastry, "Nonholonomic motion planning: Steering using sinusoids," *IEEE Trans. on Automatic Control*, vol. 38, no. 5, pp. 700–716, 1993.
11. A. C. Gelb, *Applied Optimal Estimation*, MIT Press, Cambridge, MA, 1994.

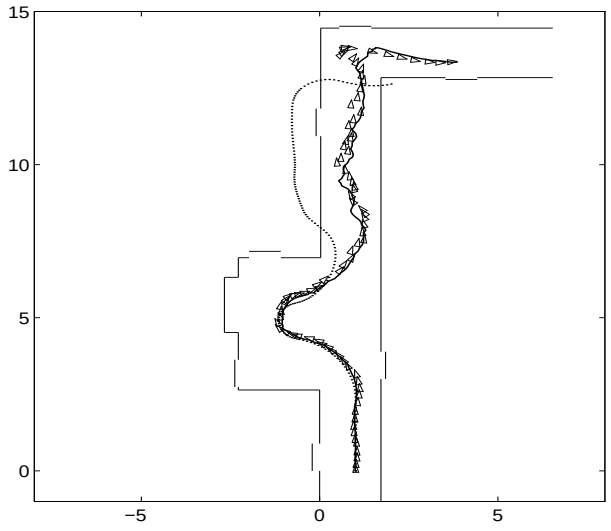

Figure 2: The actual robot positions (triangles), the odometric estimate (dotted) and the path (solid) reconstructed by our localization method. Scale is in meters.

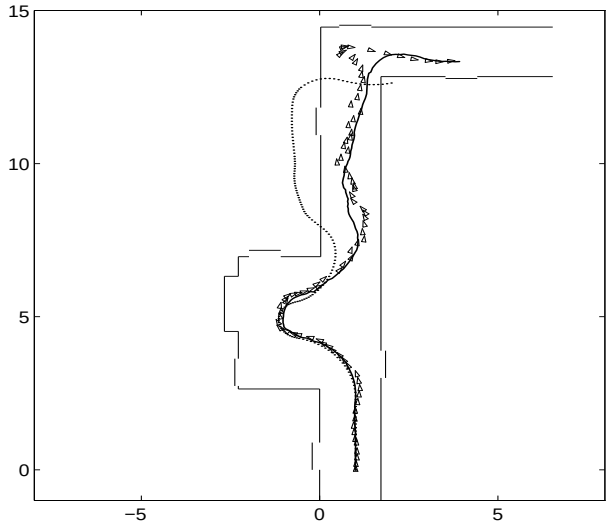

Figure 3: The actual robot positions (triangles), the odometric estimate (dotted) and the path (solid) reconstructed by a conventional EKF-based localization method. Scale is in meters.

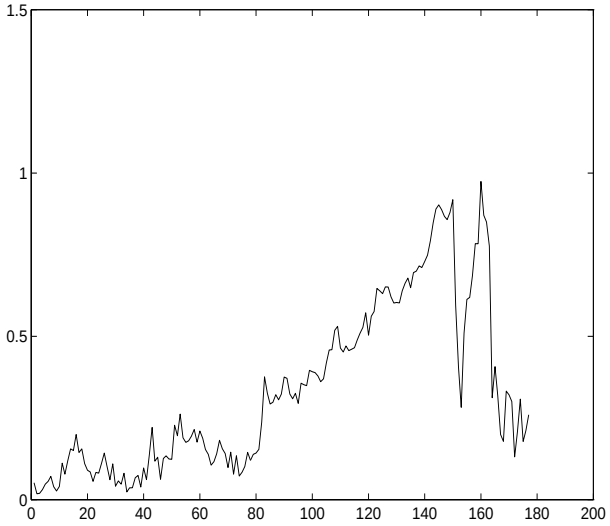

Figure 4: Cartesian position error (m) vs. sampling intervals for our localization method.

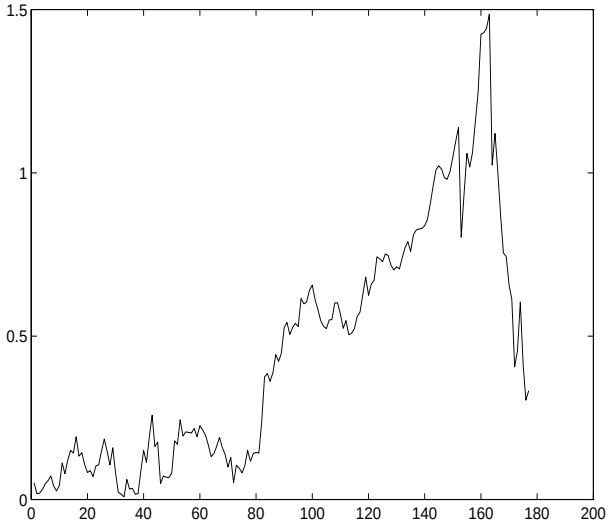

Figure 5: Cartesian position error (m) vs. sampling intervals for a conventional EKF-based localization method.

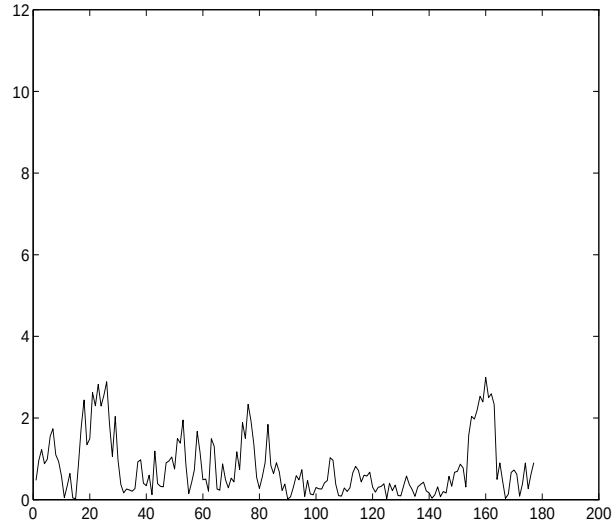

Figure 6: Orientation error (deg) vs. sampling intervals for our localization method.

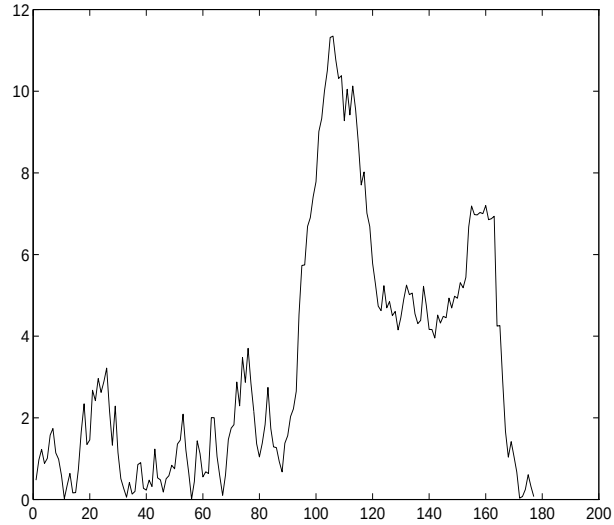

Figure 7: Orientation error (deg) vs. sampling intervals for a conventional EKF-based localization method.